Charge-Transfer Complexes of Metal Dithiolenes XXVI[+] Azobipyridinium Dications and Radical Monocations as Acceptors

Carsten Handrosch,[a] Robert Dinnebier,[b] Gennadij Bondarenko,[c] Eberhard Bothe,[d] Frank Heinemann,[a] and Horst Kisch*[a]

Keywords: Metal dithiolenes / Charge-transfer complexes / Azo compounds / Electrical conductivity / High-resolution X-ray powder diffractometry

Combination of the planar redox-active ions $[ML_2]^{2-}$ (L = mnt^{2-} = maleonitrile-1,2- dithiolate; M = Ni (**1**), Pd (**2**), Pt (**3**); $dmit^{2-}$ = 2-thioxo-1,3-dithiol-4,5-dithiolate: M = Ni (**4**), Pd (**5**) and *trans*-4,4′-azobis(1-methyl-pyridinium), ($\mathbf{a}^{2+}$) affords 1:1 ion pairs exhibiting partial and complete electron transfer as evidenced by UV-Vis and EPR spectra. Replacement of planar $\mathbf{a}^{2+}$ by a non-planar dipyridinium ketone $\mathbf{b}^{2+}$ leads to the complexes **1b** and **4b**. **1a**, **2a**, and **3a** are predominantly composed of dications and dianions while **4a**, **5a**, and **4b** are rare examples of ion pairs consisting of two radical ions. Single crystal X-ray structural analyses was performed on **4a**, $\mathbf{a}(PF_6)_2$, and $\mathbf{a}(MeSO_4)_2$ while the structure of **1a** was resolved by powder X-ray diffractometry. The latter consists of mixed stacks of planar dianions and dications forming a slipped arrangement with the centers of the two ions displaced relative to each other by 250 pm. The short interplanar distances of 340 pm are in agreement with the presence of a weak charge-transfer interaction as indicated by the corresponding absorption band at about 1400 nm. A mean reorganization energy of 0.85 ±0.04 eV is calculated from the Hush equation for complexes **1a, 2a**, and **3a**. No ion pair charge-transfer band is observable for **4a**, **5a**, and **4b**. Surprisingly, in the solid state structure of **4a** the $[Ni(dmit)_2]^-$ monoanions do not form segregated columns as found in the many ion pairs with redox inert counterions, but prefer a mixed stack arrangement as observed also for **1a.** The specific electrical conductivity of pressed powder pellets of complexes exhibiting a charge-transfer band is in the range of 2×10^{-7} to 1×10^{-5} $\Omega^{-1}cm^{-1}$, increasing with increasing driving force of electron transfer in accordance with previous results. Different to that, the conductivity of the other complexes does not depend on driving force and is much higher (2×10^{-4} to 4×10^{-4} $\Omega^{-1}cm^{-1}$).

Introduction

The control of physical properties of a solid by variation of molecular parameters is a central topic in materials science.[2] In recent work we have found that ion-pair charge-transfer (IPCT) complexes consisting of redoxactive components provide ideal conditions to study the influence of weak supramolecular CT interactions on the electrical conductivity. It was found that for class I complexes of the type $\{A^{2+}[ML_2]^{2-}\}$ wherein the acceptor A^{2+} is a planar dicationic 4,4′- or 2,2′-bipyridinium derivative and the $[ML_2]^{2-}$ donor is a planar dithiolene metalate, L = 2-thioxo-1,3-dithiol-4,5-dithiolate ($dmit^{2-}$) and maleonitrile-1,2-dithiolate (mnt^{2-}), M = Ni, Pd, Pt, the electrical conductivity (σ) of pressed powder pellets increases linearly on a logarithmic scale from 10^{-11} to 10^{-3} $\Omega^{-1}cm^{-1}$ when the driving force of electron transfer from the donor to the acceptor (ΔG_{12}) is varied from 0.7 to −0.1 eV.[3][4] As ΔG_{12} is easily obtained from the solution redox potentials of the two components, the conductivity of the solid IPCT salts can be quantitatively predicted from these molecular parameters. Although the CT interaction is very weak as indicated by the small fraction of an electron transferred from the donor to the acceptor, which is 0.01 to 1%,[5] σ varies over eight orders of magnitude. No similar correlation existed when the d^8 central metal was replaced by a d^7 ion like Co(II).[6] In addition to this strong electronic influence on the electrical properties we have shown that steric alterations like *cis*-*trans* isomerization of the acceptor component may have also a significant effect. While in the case of $[Ni(mnt)_2]^{2-}$ the σ value does not change when the counterion *trans*-DPE-Me^{2+} (Figure 1) is replaced by the *cis*-isomer, it increases by one order of magnitude for the $[Ni(dmit)_2]^{2-}$ complex.[7] This finding suggested that a controlled change of conductivity through photoisomerization may become feasible. In order to investigate whether the observed effect is a unique property of DPE-Me^{2+} or of more general importance, in the present work the acceptor was modified by replacing the bridging ethene fragment by an azo group, well-known to undergo photoisomerization. In the following we report on the synthesis, solid state structure and electrical conductivity of ion pair complexes containing the *trans*-isomer of the new acceptor DPD-Me^{2+} (Figure 1).

[+] Part XXV: See ref.[1]

[a] Institut für Anorganische Chemie der Universität Erlangen-Nürnberg
Egerlandstraße 1, D-91058 Erlangen, Germany
[b] Lehrstuhl für Kristallographie der Universität Bayreuth, Universitätsstraße 30, D-95440 Bayreuth, Germany
[c] Department of Physical Chemistry, Rostov University Zorge St. 7, 344092 Rostov-on-Don, Russia
[d] Max-Planck-Institut für Strahlenchemie, Stiftstraße 34−36, D-45470 Mülheim / Ruhr, Germany

  1434−1948/99/0808−1259 $ 17.50+.50/0

Out of the four structures investigated by X-ray analysis three of them were resolved by the conventional single crystal method and one by the more unconventional powder diffractometry.

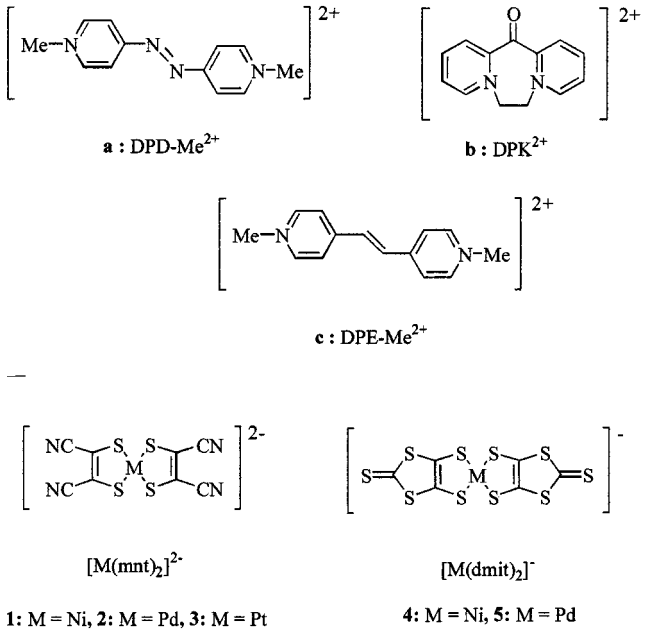

Figure 1. Isolated complexes

Results

DPD-Me(X)$_2$ [X = MeSO$_4$, PF$_6$]

The azoviologen salt **a**(MeSO$_4$)$_2$ was synthesized as described recently[8] and converted into **a**(PF$_6$)$_2$ by metathesis with NH_4PF_6. Single crystals of both salts were obtainable and their structures were solved by X-ray analysis. The observed bond lengths and angles for both compounds are equal within experimental error and therefore only the structure of **a**(PF$_6$)$_2$ × 2 (Me$_2$CO) is shortly discussed (Figure 2, Table 1) but the crystal data of **a**(MeSO$_4$)$_2$ are included in the Experimental Section. The N=N and C−N bond lengths of 123.6 and 143.5 pm agree well with the values of 123 and 141 pm reported for azobenzene[9] and with 127.3 and 143.3 pm calculated for a 4-[4-(dimethylamino)phenyl]azopyridinium salt.[10] Various attempts to isomerize $\mathbf{a}^{2+}$ failed. In all cases no change was observable in the UV-Vis spectrum upon irradiation at various wavelengths.

The cyclic voltammogram of **a**(PF$_6$)$_2$ in acetonitrile exhibits two reversible redox waves at −0.207 V and −0.536 V (vs. Ferrocene), which are assigned to the DPD-Me^{2+}/DPD-Me$^{\bullet+}$ and DPD-Me$^{\bullet+}$/DPD-Me^0 redox steps, respectively (Figure 3a). While the well-known radical cation of methylviologen [11a−d] is blue, DPD-Me$^{\bullet+}$ is deep red. It was generated in a spectroelectrochemical experiment by reduction of the dication at −0.3 V (vs. ref.). This electrolysis led to a constant absorbance at 452 nm ($\varepsilon_{452} = 4.4 \times 10^4$ M^{-1} cm^{-1}). In addition to this sharp band, a broad absorption developed in the range from 500 to 600 nm as depicted in Figure 3b.

Table 1. Selected bond lengths [pm] and angles [°] of **a**(PF$_6$)$_2$ × 2(Me$_2$CO) with estimated standard deviations in parentheses

N(1)−C(16)	147.7(4)
N(1)−C(11)	133.5(4)
N(2)−C(13)	143.5(4)
C(11)−C(12)	136.9(4)
C(12)−C(13)	138.7(4)
C(13)−C(14)	138.3(4)
C(14)−C(15)	137.0(4)
N(1)−C(15)	134.0(4)
N(2)−N(2′)	123.6(5)
C(12)−C(13)−N(2)	115.5(3)
C(14)−C(13)−N(2)	124.4(3)
N(2′)−N(2)−C(13)	113.2(3)

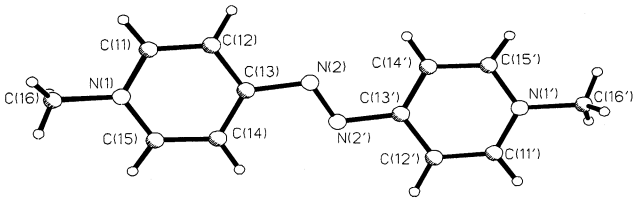

Figure 2. Molecular structure of **a**(PF$_6$)$_2$ × 2 (Me$_2$CO)

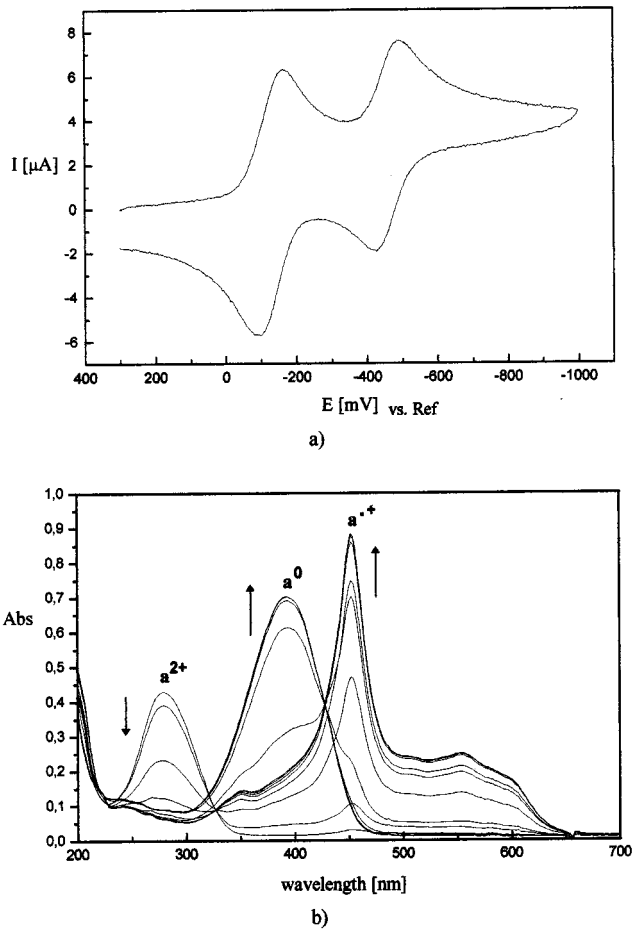

Figure 3. a) Cyclic voltammogram of **a**(PF$_6$)$_2$ in MeCN; v = 0.2 Vs^{-1}; MeCN; E vs. Ag/0.01 M $AgNO_3$; b) Spectroelectrochemistry of **a**(PF$_6$)2 in MeCN

These data agree very well with the one reported for the ethyl derivative DPD-Et$^{\bullet+}$ which was also generated electrochemically.[11c] But different to DPD-Me$^{\bullet+}$, no structural information is available for this ethyl or any other derivative. Further reduction at −0.7 V (vs. ref.) led to the yellow-colored neutral diimine with a single absorption band at 392 nm ($\varepsilon_{392} = 3.5 \times 10^4$ M^{-1} cm^{-1}). Isosbestic points are observed at 325 and 425 nm (Figure 3b).

Chemical reduction of DPD-Me^{2+} to the radical cation can be performed with $S_2O_3^{2-}$, NEt_3, Zn/HOAc, $[Zn(mnt)_2]^{2-}$, Na_2mnt or simply photochemically by dissolving **a**$(PF_6)_2$ in MeOH under diffuse daylight. The resulting red solutions were stable for several days when kept under dinitrogen at −25°C.

In agreement with the slightly twisted structure[12b] DPK^{2+} (Figure 1) is a slightly worse acceptor than DPD-Me^{2+} as indicated by the first reduction potential of −0.06 V (MeCN, vs. SCE)[3] (congruent with −0.45 V vs. ferrocene). Although the radical cation was generated electrochemically[12a] and characterized by resonance raman spectroscopy,[12b] no electronic absorption spectrum was reported. While DPK^{2+} starts absorbing only at about 400 nm, the deep red acetone solution of DPK$^{\bullet+}$, generated under dinitrogen through reduction with aqueous sodium thiosulfate, exhibits a broad maximum already at 507 nm ($\Delta\tilde{\nu}_{1/2} = 1435$ cm^{-1}).

Powder X-Ray Diffractometry of 1a

The complexes **1a** to **5a** were all precipitated by adding slowly a acetone solution of the dication to the dissolved dianion, as described recently.[3][6] All complexes gave satisfactory elemental analyses except **4a**, for which non-stoichiometric compositions of (DPD-Me)$_x$[Ni(dmit)$_2$], $x = 0.7$ to 0.9 were found (vide infra).

Since no single crystals of **1a** could be obtained, the structure was solved by powder X-ray structural analysis.[13] The resulting bond lengths suggest that the nickel component is present as dianion (Table 2). This is indicated by the observed mean Ni−S length of 219.1(4) pm, which is close to the Ni−S bond length of 217.4(2) pm in $\{MV^{2+}[Ni(mnt)_2]^{2-}\}$[14] and comparable $[Ni(mnt)_2]^{2-}$ complexes.[15] The corresponding value in $[Ni(mnt)_2]^-$ compounds is 214.3(2) pm.[16][17] Different to that, the observed N−N length of 131.2(2) pm strongly deviates both from the values of 123.6(5) and 135.5(8) pm observed for the dication (Table 1) and radical cation (Table 4), respectively, while the C−N bond length of 142.8(2) pm is not significantly different from 143.5(4) pm as found for the dication. On the other hand, the difference between the C−N and N=N length is 19.9 and 11.6 pm in DPD-Me^{2+} and **1a**, respectively, while it is negligible in DPD-Me$^{\bullet+}$. It is therefore proposed that the structure of **1a** consists of DPD-Me^{2+} and $[Ni(mnt)_2]^{2-}$ ions. These are arranged as mixed stacks (Figure 4), as also found in other class I IPCT complexes like $\{(MV)^{2+}[Ni(mnt)_2]^{2-}\}$,[14] $\{(DPE\text{-}R)^{2+}[Ni(mnt)_2]^{2-}\}$, [R = $(CH_2)_4CN$],[7] and $\{(MV)^{2+}[Pd(mnt)_2]^{2-}\}$.[18a] As observed in these structures, the two components of **1a** are slipped along the longest molecule axis by about 250 pm. Short interplanar distances are slightly below or above the corresponding sum of the van der Waals radii (Table 3).[18b,19] The average value of 340 pm is characteristic for dithiolene metalate IPCT complexes.[7][18][20]

Table 2. Selected bond lengths [pm] and angles [°] of **1a** with estimated standard deviations in parentheses

DPD-Me^{2+}		$[Ni(mnt)_2]^{2-}$	
N(3)−N(3a)	131.2(2)	Ni(1)−S(1)	219.9(4)
N(3)−C(5)	142.8(2)	Ni(1)−S(2)	218.3(4)
C(5)−C(9)	138.0(2)	S(1)−C(1)	167.8(2)
C(8)−C(9)	134.1(2)	S(2)−C(2)	174.9(2)
N(4)−C(8)	145.8(2)	C(1)−C(2)	136.0(2)
N(4)−C(7)	131.8(2)	C(1)−C(4)	153.5(2)
C(6)−C(7)	138.3(2)	C(4)−N(1)	119.4(2)
C(5)−C(6)	135.7(2)	C(2)−C(3)	147.5(2)
		C(3)−N(2)	105.6(2)
		S(1)−Ni(1)−S(2)	93.33(1)

Single Crystal X-Ray Analysis of 4a

Suitable, dark-green single crystals of **4a** × DMF were obtained by crystallization from DMF/acetone under nitrogen atmosphere. The Ni−S bond lengths of 215−216 pm indicate the presence of the monoanion $[Ni(dmit)_2]^-$[21] since a value of 221 pm is expected for the dianion (Figure 5a, Table 4).[22] This is corroborated by the characteristic electronic absorption spectra (vide infra). The structure of the cationic component in **4a** significantly differs from that of the DPD-Me^{2+} dication as indicated by the comparison of the central CNNC fragments. In the dication the C13−N2 and N2−N2′ bond lengths are 143.5(4) and 123.6(5) pm, respectively, while in **4a** the values of the corresponding C13−N2, C7−N1 and N1−N2 bonds are 134.7(8), 137.7(8) and 135.5(8) pm. Thus, while for DPD-Me^{2+} the C−N bond is about 20 pm longer than the N=N bond, no significant difference is observed for the cation present in **4a**. Accordingly, complex **4a** is composed of two radical ions, a combination hitherto unknown for dithiolene metalate−viologen ion pairs. Contrary to the structure of **1a**, the two components are slipped only marginally relative to each other. In the resulting structure one of the azo nitrogen atoms (N1) is located 362 pm perpendicular above the central nickel ion. Although the distance is much longer than 318 pm, the sum of the corresponding van der Waals radii,[18b,19] it may suggest a weak coordinative interaction and would rationalize the much smaller slipping as compared to **1a**.

Compared to the interplanar distances within **1a**, those in **4a** are remarkably longer (Table 5) and the mean value of 365 pm is in the range of interplanar anion distances as reported for $[Ni(dmit)_2]^-$ complexes with more simple countercations.[21] All values are about 20 pm longer than the sum of the corresponding van der Waals radii. If at all,

Table 3. Shortest interplanar distances in **1a**

	Ni(1a)···C(9a)	S(2a)···N(3a)	C(2a)···N(3)	C(3a)···C(5)	N(2a)···C(9)	S(1)···C(7a)
[pm]	344	337	345	334	333	344
[pm][a]	333	335	325	340	325	335

[a] sum of the corresponding van der Waals radii[19]

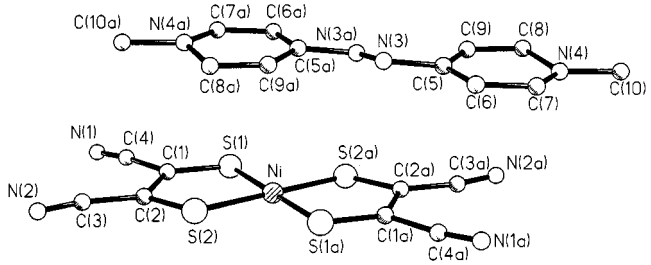

Figure 4. Molecular structure of **1a**

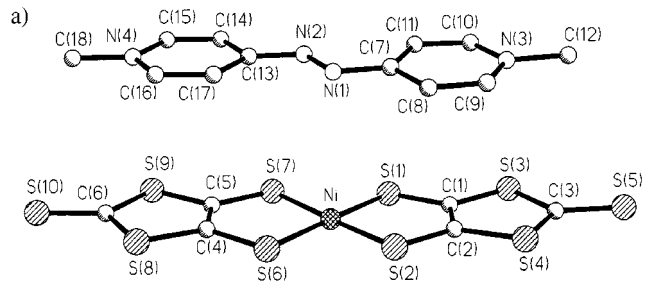

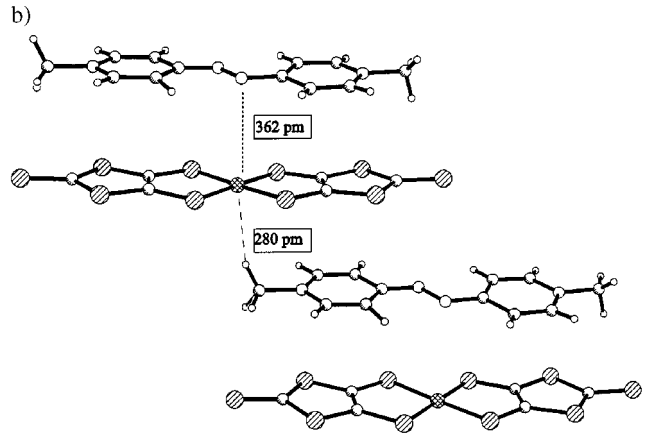

Figure 5. Molecular structure of **4a** × DMF; a) isolated ion pair, b) neighboring pairs

this points to only very weak π interactions between the two components. The presence of weak hydrogen bonding between the ion pairs is suggested by the distance of 280 pm between the methyl group hydrogen atom of DPD-Me$^{\bullet+}$ and the nickel ion; the corresponding sum of the van der Waals radii is 283 pm.

As already mentioned in the discussion of the interplanar distances, the packing structure of **4a** significantly differs from the one generally observed for $[Ni(dmit)_2]^-$ monoanions. In the latter the anions form isolated stacks

Table 4. Selected bond lengths [pm] and angles [°] of **4a** × DMF with estimated standard deviations in parentheses

DPD-Me$^{\bullet+}$	**$[Ni(dmit)_2]^-$**		
N(3)−C(10)	132.9(9)	Ni(1)−S(6)	215.5(2)
N(3)−C(9)	135.2(8)	Ni(1)−S(1)	215.6(2)
N(3)−C(12)	147.6(8)	Ni(1)−S(7)	216.3(2)
N(1)−N(2)	135.5(8)	Ni(1)−S(2)	216.7(2)
N(1)−C(7)	137.7(8)	S(1)−C(1)	172.6(6)
N(4)−C(15)	135.5(9)	S(2)−C(2)	171.8(6)
N(4)−C(16)	136.2(9)	S(3)−C(3)	171.7(7)
N(4)−C(18)	146.8(9)	S(3)−C(1)	174.2(6)
N(2)−C(13)	134.7(8)	S(4)−C(3)	173.7(6)
C(10)−C(11)	137.0(9)	S(4)−C(2)	174.3(6)
C(7)−C(11)	141.6(10)	S(5)−C(3)	165.5(6)
C(7)−C(8)	140.6(10)	S(6)−C(4)	173.2(6)
C(8)−C(9)	135.7(9)	S(7)−C(5)	172.9(6)
C(16)−C(17)	136.5(9)	S(8)−C(6)	172.7(7)
C(13)−C(17)	143.3(10)	S(8)−C(4)	173.9(5)
C(13)−C(14)	142.1(10)	S(9)−C(6)	172.0(6)
C(14)−C(15)	134.7(10)	S(9)−C(5)	175.4(5)
C(17)−C(13)−N(2)	129.3(7)	S(10)−C(6)	165.3(6)
C(13)−N(2)−N(1)	114.4(6)	C(1)−C(2)	133.9(8)
C(7)−N(1)−N(2)	114.6(6)	C(4)−C(5)	132.4(8)
N(1)−C(7)−C(11)	124.3(7)		

which are separated by the cations.[21] In contrast to that, the structure of **4a** consists of mixed anion-cation stacks as typically observed for class I IPCT complexes like MV[Ni(mnt)$_2$],[4][14] although these contain a dication and dianion. These mixed stacks are orientated along the [010] direction as depicted in Figure 6.

Within a stack each DPD-Me[Ni(dmit)$_2$] pair is slipped relative to the other by nearly half of the ion pair length resulting in a steplike arrangement (Figure 5b). Viewed perpendicular to the planar components, parallel stacks appear which are separated by the DMF molecules preventing short interstack contacts between the thioxo sulfur atoms of neighboring dithiolenes, a type of interaction which is generally observable in the many complexes where $[Ni(dmit)_2]^-$ possesses a non-redoxactive counterion.[21] On the other hand when viewed along the components planes there is no separation by solvent molecules and strong interstack interactions between the non-thioxo sulfur atoms become feasible. All corresponding distances of 331 to 362 pm are shorter than the sum of the van der Waals radii (370 pm[19]) and are characteristic for such type of S···S interactions.[21] Furthermore the distance of 331 pm is shorter than ever reported for a 3-dimensional network of $[Ni(dmit)_2]^-$ anions. The overall arrangement in the solid can be viewed as consisting of wavy sheets of distorted nickel dithiolene hexagons, hold together by strong interstack S···S interactions. The latter is typical for $[M(dmit)_2]^-$ (M = Ni, Pd, Pt) as reported for many complexes with more simple counter

Table 5. Shortest interplanar distances in **4a** × DMF

	S(2a)···C(14a)	C(2a)···C(14a)	C(2a)···C(15a)	S(4a)···C(15a)	(S3a)···N(11a)
[pm]	372	355	361	371	367
[pm][a]	350	340	340	350	335

[a] sum of the corresponding van der Waals radii[19]

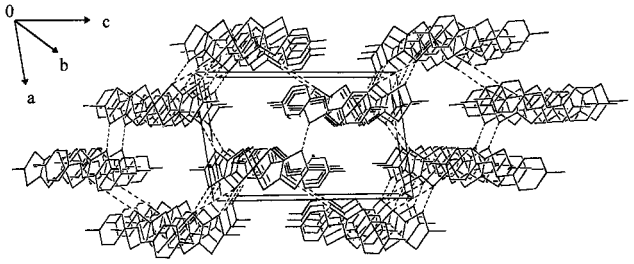

Figure 6. Crystal structure of **4a** × DMF viewed along the *b* axis [010]; dashed lines represent the interstack S···S interactions; DMF molecules are omitted

cations.[21] The ″holes″ in the $[Ni(dmit)_2]$ sheets are occupied by two DPD-$Me^{\bullet+}$ molecules. But in spite of the close packing of the radical cations, there is no evidence for a dimerization as known e.g. for $MV^{\bullet+}$ [11a,11b,23].

General Properties

Since the single-crystal structural analysis of **4a** × DMF revealed the presence of singly charged ions, electron transfer (ET) from $[Ni(dmit)_2]^{2-}$ to DPD-Me^{2+} must have occurred during the synthesis. This is thermodynamically feasible in all cases as indicated by the moderate to strong driving force of the reaction calculated from the redox potentials which were corrected for the actually involved concentrations (Table 6). Only the palladium complex **2a** and the DPK^{2+} ion pair **1b** have rather small ΔG_{12}(corr.) values of −0.08 eV and −0.07 eV, respectively. Accordingly, the UV-Vis-NIR solution absorption spectra of all DPD-Me^{2+} ion pairs except **2a** and **1b** indicate the presence of radical ions. For the mnt complexes **1a** and **3a** the diagnostic absorption of the $[Ni(mnt)_2]^-$ monoanion[24] appears at 862 nm and the DPD-$Me^{\bullet+}$ radical cation is observable at 452, 550(sh) and 600(sh) nm (Figure 7a). Based on a monoanion extinction coefficient of 8000 and 11700 M^{-1} cm^{-1} for M = Ni and Pt at 862 and 855 nm,[24] respectively, one calculates that the concentration of $[M(mnt)_2]^-$ is only 25 (**1a**) and 6% (**3a**), of the theoretical value. This suggests that the major species present is the dianion as also corroborated by the EPR spectra (vide infra). An almost complete ET can be deduced from the high absorbance of the $[Ni(dmit)_2]^-$ monoanion at 1145 nm (ε = 16250 M^{-1} cm^{-1})[25] and 1414 nm (ε = 18050 M^{-1} cm^{-1})[26] in the case of the dmit-complexes **4a**, **4b** and **5a,** respectively (Figure 7b). Small amounts of remaining dianion could form the ion pair $\{(DPD\text{-}Me^{\bullet+})_2[Ni(dmit)_2]^{2-}\}$ which would account for the non-stoichiometric composition of **4a** (vide supra). Absorptions of the radical cation are evident only in the spectrum of **5a** while they probably are superimposed by monoanion bands in the case of **4a** and **4b**.

The fact that no radical ion absorptions are observable in the spectra of **1b** and **2a** can be rationalized by the unfavorable driving force of ET (Table 6).

The diffuse reflectance spectra of **1a** and **3a** both exhibit very broad absorption bands reaching from around 700 nm to the NIR region at 2200 respectively 2400 nm (Figure 8a).

This is at much lower energy as compared to hitherto observed IPCT bands of mnt complexes which did not extend beyond λ_{max} = 1000 nm while the absorption maxima of **1a** and **3a** are around 1400 nm. As expected, the onset of this low-energy band correlates with the driving force of ET from the dianion to the dication and is therefore assigned to an IPCT transition. According to the Hush equation ($E_{IPCT} = \chi + \Delta G_{12}$) the reorganization energy χ is about the same for the DPD-Me^{2+} complexes **1a**, **2a**, and **3a** resulting in an average value of 0.85 ± 0.04 eV as calculated from the data summarized in Table 6 while 0.89 is obtained for the DPK compound **1b**. This indicates, that the different structure of the acceptor component in **1a** and **1b** does not lead to a significant change of the reorganisation energy.

The diffuse reflectance spectra of **4a**, **4b** and **5a** do not contain evidence for the presence of an IPCT band, in accordance with the absence of short interionic distances typical for π,π interactions (vide supra). The maxima at 1190 and 1490 nm can be assigned to the monoanions $[Ni(dmit)_2]^-$ and $[Pd(dmit)_2]^-$.[26] Although the low-energy tailing of **4a** and **5a** may suggest an IPCT character, its independence on the donor component excludes this possibility. More likely is the assignment to an interanion charge-transfer transition along the 3-D network of the dithiolene metalate as proposed for comparable systems.[27]

The presence of different amounts of radical ions in the mnt and dmit complexes, respectively, is suggested from the UV-Vis-NIR solution spectra. This is corroborated by ESR spectroscopy of the complexes **1a** and **4a**. The powder ESR spectra of **1a** at 77 K exhibits the three signals of the $[Ni(mnt)_2]^-$ monoanion (g_1 = 2.152, g_2 = 2.043, g_3 = 1.997) and an intense signal of the DPD-$Me^{\bullet+}$ radical cation (g = 2.006) (Figure 9a), which overlaps with the less intensive g_3 signal of the monoanion. The observed g values of the dithiolene metalate anion are in excellent agreement with the literature (g_1 = 2.160, g_2 = 2.042, g_3 = 1.998).[28] Due to the separated rhombic spectra of the monoanion and the signal of the DPD-$Me^{\bullet+}$ radical cation, it can be concluded that there are no magnetic interactions between them. For in that case only a single signal of the monoanion

Table 6. Redox potentials of the components; ΔG_{12} and E_{IPCT} of the complexes

	redox potential [V][a]			ΔG_{12} [eV]		E_{IPCT}[e] [eV]	ΔG_{12}* [eV]
	$A^{2+/+}$	$D^{-/2-}$	$D^{-/0}$	corr.[d]	uncorr.		corr.[d]
1a	+ 0.18	+ 0.23[b]	+ 1.03[b]	−0.31	+ 0.05	0.64	0.11
1b	−0.06[c]	+ 0.23[b]	+ 1.03[b]	−0.07	+ 0.29	0.82	0.19
2a	+ 0.18	+ 0.46[b]	n.d.[b]	−0.08	+ 0.28	0.79	0.18
3a	+ 0.18	+ 0.21[b]	n.d.[b]	−0.33	+ 0.03	0.60	0.10
4a	+ 0.18	−0.14[c]	+ 0.18[c]	−0.68	−0.32	–	–
4b	−0.06[c]	−0.14[c]	+ 0.18[c]	−0.43	−0.08	–	–
5a	+ 0.18	−0.02[c]	n.d.[c]	−0.56	−0.20	–	–

[a] from cyclic voltammetry in MeCN, V vs. SCE. – [b] See ref.[17] – [c] See ref.[3] – [d] calculated after correcting the redox potentials via Nernst's equation with $[D^{2-}]_0 = [A^{2+}]_0 = 10^{-3}$ M; $[D^{-}]_0 = [A^{\cdot+}]_0 = 10^{-6}$ M. – [e] onset energy as obtained from diffuse reflectance spectra (see Experimental Section)

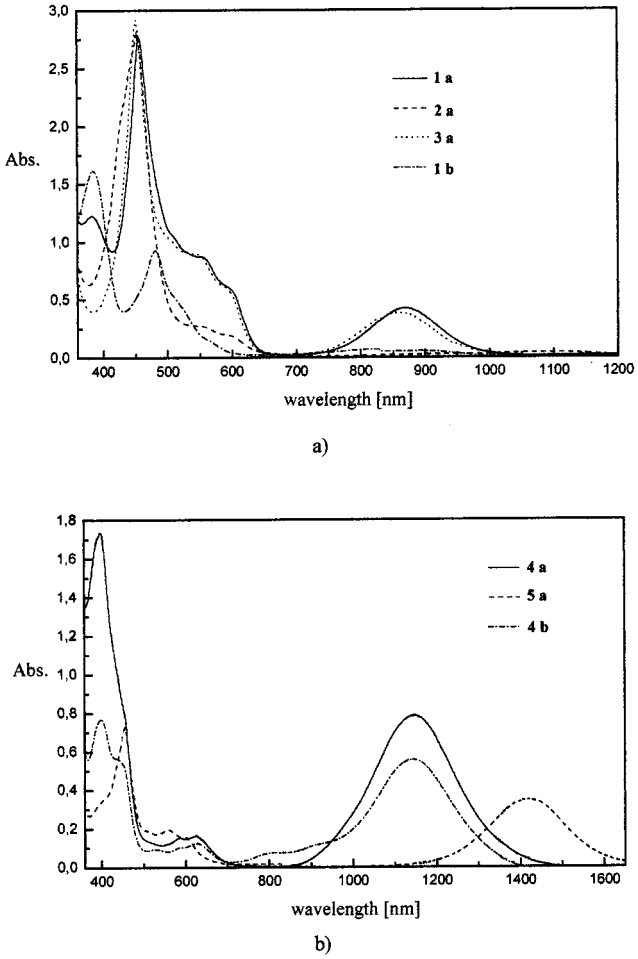

Figure 7. UV-Vis-NIR spectra in DMF; a) mnt complexes, b) dmit complexes, **5a** was measured in DMF/THF = 1 : 4 (*v*/*v*)

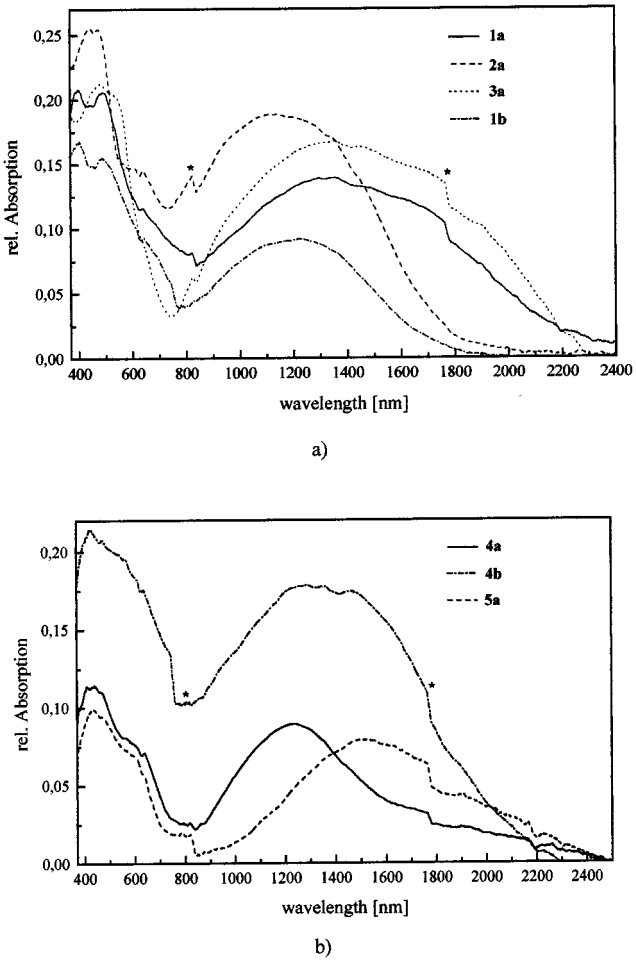

Figure 8. Diffuse reflectance spectra; a) mnt complexes, b) dmit complexes

would have been observed, as in $(NBu_4)[Ni(mnt)_2]$. This lack of interaction between the radicals is confirmed by the comparison of the spectra at room temp. and at 77 K. At both temperatures there are sharp signals of the two components, which are more intensive at the lower temperature (77 K). This is contrary to a mutual antiferromagnetic interaction between the components, in which case less intensive signals would be observed at 77 K than at room temp. From these results it is concluded that both components are magnetically diluted in the diamagnetic complex $\{DPD\text{-}Me^{2+}[Ni(mnt)_2]^{2-}\}$, which is in accordance with the electronic solution spectra showing only a small amount of the anion.

Contrary to that, the dmit complex **4a** exhibits an intensive broad signal at about $g = 2.046$ at room temperature (Figure 9b). At 77 K this apparently isotropic signal disappears, while peaks at $g_1 = 2.003$, $g_2 = 2.047$, $g_3 = 2.118$ emerge (Figure 9c). The small shoulder at the g_2 signal of the monoanion might be caused by the radical cation. These results suggest that the broad signal may be caused

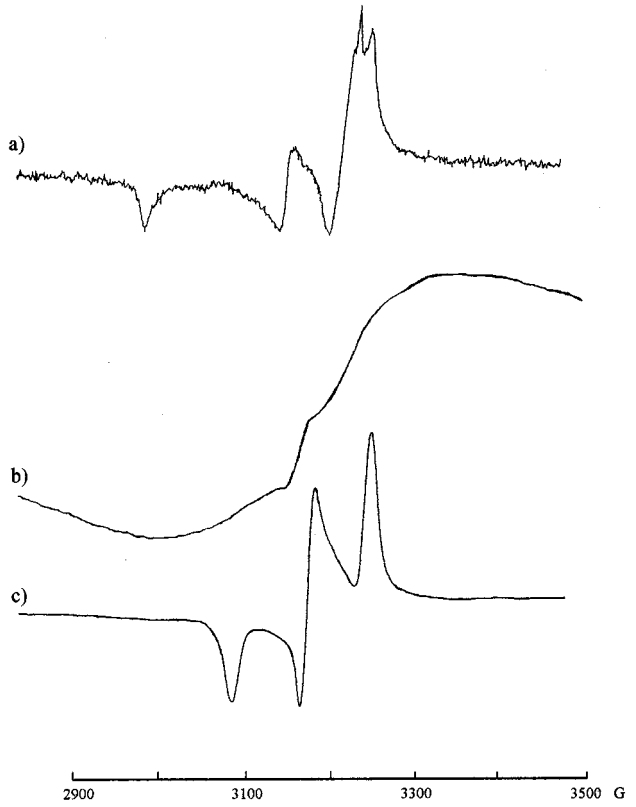

Figure 9. Powder ESR spectra; a) **1a** at 77 K, b) **4a** at room temp., c) **4a** at 77 K

by antiferromagnetic interactions between paramagnetic centers in partially oxidized (DPD-Me)[Ni(dmit)$_2$] containing also magnetically diluted monoanions. A similar broad signal was also reported for the partially oxidized (DEPZ)$_{0.35}$[Ni(dmit)$_2$], (DEPZ = diethylpyrazinium), but contrary to our results this broad signal persisted even at 77 K.[29] This antiferromagnetic interaction between the radicals in **4a** can be detected due to their much higher concentration than in **1a**. This is again in accordance with the high amounts of monoanions observed in the solution UV-spectra of the dmit complexes.

Electrical Conductivity

As expected from our previous findings that σ increases with a more negative driving force of ET when both components are planar and an IPCT band is present (class I complexes),[3] the conductivity increases from 2×10^{-7} over 4×10^{-6} to 1×10^{-5} Ω^{-1}cm^{-1} as ΔG_{12}(corr.) varies from −0.08 (**2a**) over −0.31 (**1a**) to −0.33 (**3a**) eV. The DPK^{2+} complex **1b** [ΔG_{12}(corr.) = −0.07 eV] does not follow this correlation which suggests that another factor must be responsible for this unexpected low conductivity of 1×10^{-9} Ω^{-1} cm^{-1}. Corresponding activation energies of 0.24 and 0.44 eV were measured for **1a** and **1b**, respectively, in the temperature range of 25 to 95°C. This remarkable difference is in sharp contrast to the only slightly different ΔG_{12}* (corr.) values of both complexes (**1a**: 0.11 eV; **1b**: 0.19 eV). It may be rationalized by recalling that the measured activation energy is composed of two components. The energy which is necessary for generation of conducting electrons and the energy barrier for electron transport through the crystal lattice. Since the former should be not too different as suggested by the solution ΔG_{12}*(corr.) values, it seems likely that the latter value is much higher for **1b**. The different acceptor geometries should lead to different crystal structures imposing unfavorable steric constraints for charge transport in the case of **1b**. A significant contribution of the radical species seems to be negligible since the conductivity of **3a** is about half an order of magnitude higher as compared to **1a** although the corresponding radical contents are 6 (**3a**) and 25% (**1a**, vide supra).

Contrary to the mnt complexes, the conductivity of the dmit compounds (4×10^{-4}, 3×10^{-4}, 2×10^{-4} Ω^{-1} cm^{-1} for **4a**, **4b** and **5a**, respectively) does not change significantly upon variation of the metal and acceptor. This suggests a different conduction mechanism which does not depend on electronic interaction between the two components but rather on the strong interstack S···S interactions between the monoanions (Figure 6), a well-known effect for [Ni(dmit)$_2$]$^-$ systems.[21]

Experimental Section

General Methods: Unless noted otherwise, all reactions and operations were carried out under nitrogen using standard Schlenk techniques. Solvents were dried and distilled before use. Spectra were recorded with the following instruments: NMR: Jeol FT-JNM-GX 270, EX 270 and Lambda LA 400. − ^{1}H NMR: The protio-solvent signal was used as an internal reference. Chemical shifts are quoted on the δ scale relative to tetramethylsilane. − ESR spectra were measured on a Radiopan 2543 spectrometer working in X band. − Elemental analyses: Carlo−Erba EA 1106 and 1108. − UV/Vis: Shimadzu UV-3101 PC. − Electrochemical investigations were performed with a three electrode cell with a Ag/0.01 M $AgNO_3$ reference, Pt counter and 2-mm diameter glassy carbon (CV) or Pt-gauze (spectroelectrochemistry) working electrode. Sample solutions were 4×10^{-4} M and TBA(PF$_6$) (10^{-1} M) was the supporting electrolyte. Potentials were referred to *Fc*/*Fc*$^+$ which was added to the solution as internal standard at the end of the measurement prior to the last scan. − For diffuse reflectance measurements the substances were spread on a corundum carrier (Ceram Tec) which also served as reflectance standard. The spectrometer was equipped with an intergrating shere unit. The onset of the absorption band of lowest energy was determined according to the method by Karvaly and Hevesi, originally developed for inorganic semiconductors,[30] which is independent on the sample concentration. Within the linear decrease of absorption on the low-energy side of the band, 5−6 points are selected and the term $[F(R_\infty)h\nu]^2$, with $F(R_\infty) = (1 - R_\infty)^2/2\ R_\infty$ (Kubelka−Munk function) is calculated for each of them. A plot of the first term vs. $h\nu$ affords a straight line which intersects the abscissa at the value E_{IPCT}. − Conductivity: Specific resistivities were measured for compacted pellets at ambient conditions by the conventional two-probe method as described previously.[3] Average values are given as obtained from 3−4 powder pellets; the mean deviation in these measurements was ± 18%. Activation energies E_a were measured in the range of 25−95°C at 5−6 temperatures in a thermostated oil

bath.[3] Arrhenius plots of log σ vs. $1/T$ exhibited excellent linearity with regression coefficients of 0.99 or better.

Powder X-ray Diffraction: For the powder X-ray diffraction experiments, several samples were sealed in glass capillaries (Hilgenberg glass no.50) of 0.5 mm diameter. High resolution powder diffraction data were collected at room temperature at the SUNY X3B1 beamline at the National Synchrotron Light Source, Brookhaven National Laboratory (Figure 10).

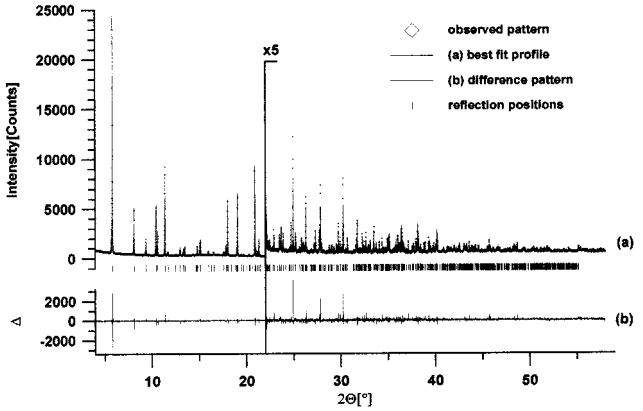

Figure 10. Rietveld plot of monoclinic **1a**. The asymmetric unit contains 23 atoms (17 non-hydrogen atoms). The spikes in the difference curve are the same as in the leBail type of fit and can be attributed to some anisotropical peak broadening which has not been refined.

X-rays of wavelength 1.14946(2) Å were selected by a double Si(111) monochromator. Wavelength and zero-point shift were determined from 8 well-defined reflections of the NIST1976 flat plate alumina standard. The diffracted beam was analyzed with a Ge(111) crystal and detected with a Na(Tl)I scintillation counter with a pulse-height discriminator in the counting chain. The incoming beam was monitored by an ion chamber for normalization for the decay of the primary beam. In this parallel beam configuration, the resolution is determined by the analyzer crystal instead of by slits. Data were taken for 3.3 s at each 2Θ from 2° to 56.805° 2Θ, for 4.3 s at each 2Θ from 40° to 48.3540° 2Θ and for 6.3 s at each 2Θ from 40° to 58.055° 2Θ in steps of 0.005° 2Θ during 2.5 GeV operation (max. 350 mA current). The three data sets were added up and normalized against 10^6 monitor counts.

Although Θ scans did not show serious crystallite size effects, the sample was spinned around the Θ axis during measurement for better statistics. Low angle diffraction peaks from (DPD-Me)[Ni(mnt)$_2$] showed strong asymmetry due to axial divergence and had a FWHM of 0.011° 2Θ, not significantly broader than the resolution of the spectrometer.

The diffraction pattern could be indexed based on a triclinic lattice using the program ITO.[31] The number of formula units per unit cell (Z) was found by geometrical considerations. Since Z was equal to 1 and the DPD-Me^{2+} cation as well as the [Ni(mnt)$_2$]$^{2-}$ ion contain a center of inversion, P-1 was chosen as the most likely space group, which was later confirmed by Rietveld refinement. A Le-Bail fit[32] using the program GSAS[33] worked well to extract 728 reflections up to 57.7° 2Θ. The peak profile function was modeled using a multiterm Simpson′s rule integration of the pseudo-Voigt function.[34] The strong asymmetry in the low-angle region was modeled by a lately implemented function[35] which accounts for the asymmetry due to axial divergence, leading to an strongly improved fit and therefore better profile R factors. Mainly because of the well-resolved peaks over the entire powder pattern, a minor non-constant shift of the peak positions was detected, which could be attributed to a small shift of wavelength. This effect could be satisfactory described by refining an additional sin Θ-depending term in addition to the zero point. A manual fit background using the program GUFI[36] was used in combination with a refinable 4-term cosine-series. The final profile agreement factors obtained were R-p = 5.35% and R-wp = 7.02%.

For the determination of the structure, two different procedures were used. In a direct method approach, the previously extracted intensities were used as input for the program SIRPOW92.[13c] It was possible to detect almost the entire [Ni(mnt)$_2$]$^{2-}$ anion and some fragment of the DPD-Me^{2+} cation. Alternatively, refinable starting parameters for the position and the orientation of the two independent molecules could also be derived from the single-crystal structure determination of the similar compound (MV)-[Ni(mnt)$_2$].[14] For the consecutive Rietveld refinements[37] in GSAS, all background, lattice and profile parameters obtained by the Lebail type of fit were fixed.

Since the shape of the two distinct molecules is known in very narrow limits, this additional information was used to stabilize the refinement by setting up rigid bodies derived from similar structures. Since both, the [Ni(mnt)$_2$]$^{2-}$ anion and DPD-Me^{2+} cation were located on a center of inversion, this reduced the number of refinable parameters for both molecules from 24 positional to 3 rotational parameters each. In order to allow the molecules to relax, the length, the width and in case of the [Ni(mnt)$_2$]$^{2-}$ anion also some out of plane bending of the outer atoms were refined as additional parameters. The refinement converged to a R-Bragg value around 15%.

Due to the high quality of the powder data, all (non-hydrogen) positional parameters remained very close to their rigid-body positions after turning them loose in a final cycle of refinement. Both molecules can be regarded as flat within the error limits. It was also possible to refine individual temperature factors. The final R values were R-p = 6.18%, R-wp = 8.47% and R-F = 7.53%, referring to the Rietveld criteria of fit for profile, weighted profile, and structure factor, respectively, defined in ref.[13a] Esd′s are a factor of six larger than Rietveld statistical estimates, as discussed in ref.[13a]

Single-Crystal X-ray Structure Analyses: Intensity data for the structural analyses of **a**(MeSO$_4$)$_2$, **a**(PF$_6$)2 × 2 (Me$_2$CO) and **4a** × DMF were collected on an automatic four-circle diffractometer (Siemens P4) at 200 K using Mo-K_α radiation (graphite monochromator). Data were corrected for Lorentz and polarization effects. In case of **4a** × DMF a semi-empirical absorption correction has been carried out. For **a**(MeSO$_4$)$_2$ and **a**(PF$_6$)2 × 2-(Me$_2$CO) absorption effects have been neglected. The structures were solved by direct methods and refined using full-matrix least-squares methods on F^2 (SHELXTL 5.03).[38] All non-hydrogen atoms with anisotropic displacement parameters. Hydrogen atom positions were taken from a difference fourier synthesis (exept for the H atoms of the DMF molecules in **4a** × DMF, which were geometrically positioned) and either refined isotropically [**a**(MeSO$_4$)$_2$, **a**(PF$_6$)2 × 2(Me$_2$CO)] or refined with a fixed isotropic displacement parameter (**4a** × DMF).

Orange platelets of **a**(MeSO$_4$)$_2$ were obtained when a saturated solution in methanol was layered with the same volume of acetone and allowed to cool from 20 to −20°C.

Long, orange-colored platelets of **a**(PF$_6$)2 × 2 (Me$_2$CO) were obtained when a saturated solution in acetone was layered with the same volume of 2-propanol and allowed to cool from 20 to −20°C.

Table 7. Selected crystallographic data of **a**$(MeSO_4)_2$, **a**$(PF_6)_2 \times 2\ (Me_2CO)$, **1a**, and **4a** × DMF

compound	**a**$(MeSO_4)_2$	**a**$(PF_6)_2 \cdot 2\ (Me_2CO)$	**1a**	**4a** · DMF
emp. formular	$C_{14}H_{20}N_4O_8S_2$	$C_{18}H_{26}F_{12}N_4O_2P_2$	$C_{20}H_{14}N_8NiS_4$	$C_{21}H_{21}N_5NiOS_{10}$
M_r [g/mol]	436.07	620.37	553.31	738.74
crystal size [mm]	0.40 × 0.30 × 0.30	0.60 × 0.42 × 0.16	–	0.42 × 0.35 × 0.15
F (000)	456	632	282	756
space group	$P2_1/n$	$P2_1/m$	P-1	P-1
cryst. syst.	monoclinic	monoclinic	triclinic	triclinic
a [pm]	621.60(12)	978.9(1)	818.816(3)	979.8(2)
b [pm]	1500.0(3)	1111.2(2)	1143.430(5)	1033.1(2)
c [pm]	1077.7(2)	1287.4(1)	635.682(3)	1535.0(3)
α [°]	90.0	90.0	96.64540(30)	78.19(1)
β [°]	106.41(3)	107.09(1)	93.00920(30)	80.29(1)
γ [°]	90.0	90.0	82.2175(4)	80.58(1)
V [nm^3]	0.9639(3)	1.3397(2)	5.85309(4)	1.4856(5)
Z	2	2	1	2
$D_{calcd.}$ [g/cm^3]	1.504	1.538	1.570	1.651
μ [mm^{-1}]	0.327	0.269	–	1.383
diffractometer	Siemens P4	Siemens P4	Huber 2-circle	Siemens P4
radiation [pm]	Mo-K_α (λ = 71.073)	Mo-K_α (λ = 71.073)	114.946(2)	Mo-K_α (λ = 71.073)
temperature [K]	200	200	295	200
scan technique	ω scan	ω scan	Θ/2Θ	ω scan
2Θ range [°]	4.7–54.2	4.0–54.0	2.0–58.06	4.0–54.0
scan speed [°/min]	3.00–30.00	6.00–40.00	11.00–21.00	8.00
meas. reflections	3580	3976	740	7612
indep. reflections	2110	3079	–	6458
$R_{int.}$ [%]	2.89	2.83	7.53	4.82
obsd. reflections	1336	2057	–	3283
σ criterion	$F \geq 4\ \sigma\ (F)$	$F \geq 4\ \sigma\ (F)$	–	$F \geq 4\ \sigma\ (F)$
R; R_w [%]	5.23; 13.60	6.03; 17.07	6.18; 8.47[a]	5.82; 16.07
refined parameters	168	284	66	387

[a] As defined in ref.[13a]

Dark-green platelets of **4a** × DMF were obtained when a saturated solution in $DMF_{abs}/MeOH_{abs}$ (v/v = 1:3) was allowed to cool slowly from 80 to −20°C.

Syntheses: 4,4′-Azopyridine,[39] DPD-Me$(MeSO_4)_2$ **a**$(MeSO_4)_2$,[8] DPK$(PF_6)_2$ **b**$(PF_6)_2$,[40] $(NBu_4)_2$[Ni$(mnt)_2$],[20] $(NBu_4)_2$[Pd$(mnt)_2$], $(NBu_4)_2$[Pt$(mnt)_2$],[25] $(NBu_4)_2$[Ni$(dmit)_2$] and $(NBu_4)_2$[Pd$(dmit)_2$][41] were prepared according to literature methods. – 4,4′-Azopyridine has been chromatographed prior to use on silica gel (eluent: acetone/petroleum ether/ethyl acetate, 1:3:1) under air. Until noted otherwise all syntheses were carried out under inert gas atmosphere in absolute solvents.

a$(PF_6)_2$: This synthesis was carried out under air. 1.5 g (8.16 × 10^{-3} mol) of 4,4′-azopyridine were dissolved in 36 mL of dimethylsulfate. An orange-colored precipitate was formed after 2 min and stirring at ambient temperature was continued for half an hour. The separated precipitate was dissolved in 500 mL of methanol/ethanol/acetone (v/v = 2 : 2 : 1) and 2.85 g (17.5 × 10^{-3} mol) of NH_4PF_6 in 30 mL of water/methanol (v/v = 1 : 1) were added to the dark-orange solution. After storing in the refrigerator for 2 h, the small orange-colored needles were filtered off through a filter funnel, washed twice with 10 mL of ethanol and dried in vacuo. Yield: 3.6 g (88%) of **a**(PF_6), orange-colored needles. – UV/Vis (acetone): λ_{max} = 280 nm, 450. – ^{1}H NMR (270 MHz, [D$_6$]acetone): δ = 4.80 [d, 6 H, NCH_3], 8.67 [d, 4 H, *3,3′*-, *5,5′*-aromatic H], 9.45 [d, 4 H, *2,2′*-, *4,4′*-aromatic H]. – $C_{12}H_{14}N_4P_2F_{12}$ (504.0): calcd. C 28.57, H 2.80, N 11.11; found C 28.61, H 2.77, N 11.01.

1a: A solution of 201.6 mg (0.40 × 10^{-3} mol) of **a**$(PF_6)_2$ in 40 mL of acetone was added dropwise to 330.0 mg (0.40 × 10^{-3} mol) of $(NBu_4)_2$[Ni$(mnt)_2$] in 50 mL of acetone. Rapidly a dark-brown precipitate was formed which was collected by filtration after standing in the refrigerator for 2 h. The microcrystalline solid was carefully washed both with 10 mL of methanol and acetone and dried in vacuo.Yield: 215 mg (97%) of **1a**, dark-brown microcrystalline powder. UV/Vis (solid): λ_{max} = 398 nm, 474, 1300. – UV/Vis (DMF): λ_{max} = 382 nm, 456, 550, 600, 872. – $C_{20}H_{14}N_8NiS_4$ (553.31): calcd. C 43.41, H 2.55, N 20.25, S 23.18; found C 43.27, H 2.46, N 20.16, S 23.00.

1b: To a solution of 741 mg (0.90 × 10^{-3} mol) of $(NBu_4)_2$[Ni$(mnt)_2$] in 30 mL of acetone, a solution of 453 mg (0.90 × 10^{-3} mol) of **b**$(PF_6)_2$ in 150 mL of acetone was added dropwise. Immediately a dark-brown solid started to precipitate and stirring was carried on for 45 min and the mixture was kept in the refrigerator for 3.5 h. The precipitate was filtered off through a filter funnel, washed three times with 5-mL portions of acetone and dried in vacuo. Yield: 450 mg (91%) of **1b**, dark-brown powder. UV/Vis (solid): λ_{max} = 410 nm, 489, 641(sh), 1224. – UV/Vis (DMF): λ_{max} = 385 nm, 481, 816. – $C_{21}H_{12}N_6NiOS_4$ (550.70): calcd. C 45.76, H 2.18, N 15.25, S 23.24; found C 45.84, H 1.99, N 15.24, S 23.83.

2a: A solution of 355 mg (0.70 × 10^{-3} mol) of **a**$(PF_6)_2$ in 50 mL of acetone was added dropwise within 30 min to 610 mg (0.70 × 10^{-3} mol) of $(NBu_4)_2$[Pd$(mnt)_2$] in 90 mL of acetone. Rapidly an olive-brown, microcrystalline precipitate was formed. Stirring was continued for half an hour, after which the precipitate was collected by filtration, washed twice with 10 mL of acetone and dried in vacuo. Yield: 410 mg (98%) of **2a**, olive-brown microcrystalline powder. UV/Vis (solid): λ_{max} = 350 nm, 449, 469, 639, 1124. – UV/Vis (DMF): λ_{max} = 452 nm, 550, 600, 1100. – $C_{20}H_{14}N_8PdS_4$ (600.04): calcd. C 39.97, H 2.33, N 18.65, S 21.32; found C 39.79, H 2.36, N 18.51, S 21.31.

3a: A solution of 86 mg (0.17 × 10^{-3} mol) of **a**$(PF_6)_2$ in 17 mL of acetone was added within 20 min dropwise to a solution of 166 mg (0.17 × 10^{-3} mol) of $(NBu_4)_2$[Pt$(mnt)_2$] in 26 mL of acetone. Rapidly an violet-brown, microcrystalline precipitate was formed. Stir-

ring was continued for 30 min, after which the precipitate was filtered off. After washing with 5 mL of acetone, the complex was recrystallized from 5 mL of DMF. After two weeks in the refrigerator the black, microcrystalline product was filtered off, washed twice with 2 mL of acetone and dried in vacuo. Yield: 85 mg (73%) of **3a**, dark-brown microcrystalline powder. UV/Vis (solid): λ_{max} = 486 nm, 1357. – UV/Vis (DMSO): λ_{max} = 460 nm, 550(sh), 600(sh), 870. – $C_{20}H_{14}N_8PtS_4$ (689.70): calcd. C 34.83, H 2.05, N 16.25, S 18.59; found C 34.71, H 1.85, N 16.10, S 18.50.

(DPD-Me)$_x$[Ni(dmit)$_2$]; x = 0.7–1.0 (4a): To a cooled (−35°C) solution of 280 mg (0.30×10^{-3} mol) of $(NBu_4)_2[Ni(dmit)_2]$ in 80 mL of acetone was added dropwise within 20 min a cooled (−30°C) solution of 150 mg (0.30×10^{-3} mol) of **a**$(PF_6)_2$ in 50 mL of acetone. During the addition the temperature of the mixture was kept between −35 and −30°C. The brown product started to precipitate immediately. The mixture was then cooled down to −40°C and the precipitate was filtered off as fast as possible (25 min). During the filtration the mixture was allowed to warm up to 0°C. After washing once with 5 mL of acetone and twice with 5 mL of methanol at room temp. the product was dried in vacuo.Yield: 185 mg (93%) of **4a**, dark-brown microcrystalline powder. UV/Vis (solid): λ_{max} = 440 nm, 1243. – UV/Vis (DMF): λ_{max} = 399 nm, 584, 626, 1145. – $C_{18}H_{14}N_4NiS_{10}$ (664.70): calcd.(x = 1.0) C 32.50, H 2.11, N 8.42, S 48.14; found C 32.56, H 2.29, N 8.30, S 47.56.; these values could not be reproduced, two new syntheses gave the following results: $C_{16.8}H_{12.6}N_{3.6}NiS_{10}$ (643.30): calcd.(x = 0.9) C 31.34, H 1.96, N 7.83; found C 31.10, H 1.43, N 8.03; and $C_{15.6}H_{11.2}N_{3.2}NiS_{10}$ (621.90): calcd.(x = 0.8) C 30.10, H 1.80, N 7.20; found C 29.92, H 1.72, N 6.92, respectively.

4b: To a solution of 720 mg (0.77×10^{-3} mol) of $(NBu_4)_2[Ni(dmit)_2]$ in 62 mL of acetone, a solution of 286 mg (0.77×10^{-3} mol) of **b**$(Br)_2$ in 11 mL of acetone/water (v/v = 2:1) was added dropwise. Immediately a grey solid started to precipitate and stirring was carried on for 30 min and the mixture was kept in the refrigerator overnight. The precipitate was filtered off through a filter funnel, washed three times with 5-mL portions of acetone and once with 5 mL of water and dried in vacuo. Yield: 485 mg (95%) **4b**, dark-grey powder. UV/Vis (solid): λ_{max} = 410 nm, 570 (sh), 600 (sh), 1300. – UV/Vis (DMF): λ_{max} = 400 nm, 450 (sh), 630 (sh), 800 (sh), 900 (sh), 1140. – $C_{19}H_{12}N_2NiOS_{10}$ (662.70): calcd. C 34.40, H 1.81, N 4.23, S 48.29; found C 34.77, H 1.86, N 4.25, S 47.54.

5a: A solution of 150 mg (0.30×10^{-3} mol) of **a**$(PF_6)_2$ in 20 mL of acetone was added dropwise within 20 min to a solution of 296 mg (0.30×10^{-3} mol) of $(NBu_4)_2[Pd(dmit)_2]$ in 63 mL of acetone/methanol (v/v = 20 : 1). Rapidly, brown microcrystals started to precipitate. Stirring was carried on for 30 min. After standing in the refrigerator overnight, the product was filtered off, washed twice with 5 mL of acetone and dried in vacuo. Yield: 65 mg (30%) of **5a**, dark-grey microcrystalline powder. UV/Vis (solid): λ_{max} = 434 nm, 1529. – UV/Vis (DMF/THF = 1:4): λ_{max} = 320 nm, 456, 559, 610, 1414. – $C_{18}H_{14}N_4PdS_{10}$ (712.40): calcd. C 30.32, H 1.97, N 7.86, S 44.92; found C 30.60, H 2.10, N 7.78, S 43.34.

Acknowledgments

This work was supported by Volkswagen-Stiftung (C. H., H. K.), Deutsche Forschungsgemeinschaft (R. D.), and Deutscher Akademischer Auslandsdienst (G. B.). Part of the work was carried out at the National Synchrotron Light Source at Brookhaven National Laboratory, which is supported by the U.S. Department of Energy, Division of Materials Sciences and Division of Chemical Sciences. The SUNY X3 beamline at NSLS is supported by the Division of Basic Energy Sciences of the U.S. Department of Energy under grant DE-FG02−86ER45231.

[1] U. Ammon, C. Chiorboli, W. Dümler, G. Grampp, F. Scandola, H. Kisch, *J. Phys. Chem. A* **1997**, *101*, 6876−6882.
[2] [2a] G. J. Ashwell (Ed.), *Molecular Electronics,* Research Studies Press Ltd., Taunton, Somerset, England, **1992**. – [2b] F. L. Carter (Ed.), *Molecular Electronic Devices*, Marcel Dekker Inc., New York, Basel, **1992**.
[3] I. Nunn, B. Eisen, R. Benedix, H. Kisch, *Inorg. Chem.* **1994**, *33*, 5079−5085.
[4] [4a] H. Kisch, *Coord. Chem. Rev.* **1993**, *125*, 155−172. – [4b] H. Kisch, *Coord. Chem. Rev.* **1997**, *159*, 385−396.
[5] As estimated from the parameter α^2 obtained from application of the Hush model (see ref.[3]).
[6] G. Schmauch, F. Knoch, H. Kisch, *Chem. Ber.* **1995**, *128*, 303.
[7] G. Schmauch, F. Knoch, H. Kisch, *Chem. Ber.* **1994**, *127*, 287−294.
[8] J. E. Rockley, L. A. Summers, *Aust. J. Chem.* **1981**, *34*, 2683−2686.
[9] H. Rau, *Angew. Chem*. **1973**, *85*, 248−258.
[10] C. H. Huang et al. *J. Phys.Chem.***1996**, *100*, 15525−15531.
[11] [11a] E. M. Kosower, J. L. Cotter, *J. Am. Chem. Soc.* **1964**, *86*, 5524−5527. – [11b] M. Wolszczak, Cz. Stradowski, *Radiat. Phys. Chem.* **1989**, *33*, 355−359. – [11c] S. Hünig, D. Scheutzow, P. Cársky, R. Zahradnik, *J. Phys. Chem.* **1971**, *75*, 335−339. – [11d] T. Watanabe, K. Honda, *J. Phys. Chem.***1982**, *86*, 2617−2619.
[12] [12a] A. L. Black, L. A. Summers, *J. Chem. Soc. (C)* **1970**, 2394−2395. – [12b] D. J. Barker, L. A. Summers, R. P. Cooney, G. R. Clark, C. E. F. Rickard, *J. Mol. Struct.* **1987**, *159*, 265−278.
[13] [13a] J. I. Langford, D. Louër, *Rep. Prog. Physics* **1996**, *59*, 131−234. – [13b] N. Masciocchi, A. J. Sironi, *J. Chem. Soc. Dalton Trans.* **1997**, 4643−4650. – [13c] C. Giacovazzo, *Acta Cryst.* **1996**, *A52*, 331−339. – [13d] K. D. M. Harris, M. Tremayne, *Chem. Mater.* **1996**, 2554−2570. – [13e] U. M. Schmidt, R. E. Dinnebier, *J. Appl. Cryst.* **1998**, in press.
[14] H. Kisch, A. Fernández, Y. Wakatsuki, H. Yamazaki, *Z. Naturforsch.* **1985**, *40b*, 292−297.
[15] B.-Z. Shan, X.- M. Zhang, X.- Z. You, H.- K. Fun, K. Sivakumar, *Acta Cryst*. **1996**, *C52*, 1148−1150.
[16] J. Morgado, I. C. Santos, L. F. Veiros, R. T. Henriques, M. T. Duarte, M. Almeida, L. Alcacer: *J. Mater. Chem.* **1997**, *7*, 2387−2392.
[17] J. A. McCleverty, *Prog. Inorg. Chem.* **1968**, *10*, 49−219.
[18] [18a] M. Lemke, F. Knoch, H. Kisch, *Acta Cryst.* **1993**, *C49*, 1630−1632. – [18b] To take distances lower than the sum of the van der Waals radii as criterion is not unambiguous since weak electrostatic forces reach much longer. e.g. T. Steiner, *J. Chem. Soc. Chem. Commun*. **1997**, 727.
[19] A. Bondi, *J. Phys. Chem.* **1964**, *68*, 441−451.
[20] E. Billig, R. Williams, I. Bernal, J. H. Waters, H. Gray, *Inorg. Chem.* **1964**, *3*, 663−666.
[21] [21a] O. Lindqvist, L. Andersen, J. Sieler, G. Steinmecke, E. Hoyer, *Acta Chem. Scand. A* **1982**, *36*, 855−856. – [21b] R. Kato, T. Mori, A. Kobayashi, Y. Sasaki, H. Kobayashi, *Chem. Lett.* **1984**, 1−4. – [21c] L. Valade, J.-P. Legros, M. Bousseau, P. Cassoux, *J. Chem. Soc. Dalton Trans.* **1985**, 783−794. – [21d] D. Mentzafos, A. Hountas, A. Terzis, *Acta Cryst.* **1988**, *C44*, 1550−1553. – [21e] P. Cassoux, L. Valade, *Coord. Chem. Rev.* **1991**, *110*, 115−160. – [21f] Kochurani, H. B. Singh, J. P. Jasinski, E. S. Paight, R. J. Butcher, *Polyhedron* **1997**, *16*, 3505−3510. –
pf1[g] Sh. Sun, P. Wu, D. Zhu, *Synth. Met.* **1997**, *88*, 243−247.
[22] O. Lindqvist, L. Sjölin, J. Sieler, G. Steinmecke, E. Hoyer, *Acta Chem.Scand. A* **1979**, *33*, 445−448.
[23] [23a] C. L. Bird, A. T. Kuhn, *J. Chem. Soc. Rev.* **1980**, *10*, 49−82. – [23b] H. Wolkers, R. Stegmann, G. Frenking, K. Dehnicke, D. Fenske, G. Baum, *Z. Naturforsch.* **1993**, *48 b*, 1341−1347.
[24] A. Davison, N. Edelstein, R. H. Holm, A. H. Maki, *Inorg.Chem*. **1963**, *6*, 1227−1232.
[25] A. Davison, R. H. Holm, *Inorg. Synth.* **1966**, 8−26.
[26] B. Eisen, *Doctoral Thesis*, University of Erlangen-Nürnberg, **1995**.
[27] A. E. Underhill et al., *J. Phys. Cond. Matter.* **1991**, *3*, 933−954.

[28] R. D. Schmitt, A. H. Maki, *J. Am. Chem. Soc.* **1968**, *90*, 2288−2292.
[29] Y. Sakamoto, G. E. Matsubayashi, T. Tanaka, *Inorg. Chim. Acta* **1986**, *113*, 137− 141.
[30] B. Karvaly, I. Hevesi, *Z. Naturforsch.* **1971**, *26a,* 245.
[31] J. W. Visser, *J. Appl. Cryst.* 1969, *2*, 89−95.
[32] A. leBail, H. Duroy, J. L. Fourquet, *Mat. Res. Bull.* **1988**, *23*, 447−452.
[33] A. C. Larson, R. B. Von Dreele, *Los Alamos National Laboratory Report* LAUR, **1990**, 86−748.
[34] P. Thompson, D. E. Cox, J. B. Hastings, *J. Appl. Cryst.* **1987**, *20*, 79.
[35] L. W. Finger, D. E. Cox, A. P. Jephcoat, *J. Appl. Cryst.* **1994**, *27*, 892.
[36] R. E. Dinnebier**,** Dinnebier, GUFI*, a program for measurement and evaluation of powder pattern*: Heidelberger Geowiss. Abh. 68, ISBN 3−89257−067−1, 1993.
[37] H. M. Rietveld, *J. Appl. Cryst.* **1969**, *2*, 65−71.
[38] SHELXTL 5.03 for Siemens Crystallographic Research Systems, Copyright **1995** by Siemens Analytical X-ray Instruments Inc., Madison, WI, USA.
[39] N. Campbell, A. W. Henderson, D. Taylor, *J. Chem. Soc.* **1953**, 1281−1285.
[40] [40a] A. L. Black, L. A. Summers, *J. Chem. Soc. (C)* **1970**, 2394 f. – [40b] R. F. Homer, T. E. Tomlinson, *J. Chem. Soc.* **1960**, 2498 ff.
[41] G. Steinmecke, H. J. Sieler, R. Krimse, E. Hoyer, *Phosphorus and Sulfur* **1979**, *7*, 49.

Received February 11, 1999
[I99049]